Electronic supplementary information:

Fused Perylene Diimide-Based Polymeric Acceptors for All-Polymer Solar Cells with High Open-Circuit Voltage

Lei Wang,[a] Ming Hu,[a] Xia Liu,[a] Youdi Zhang,[a] Yue Liu,[a] Zhongyi Yuan,[a,*] Xiaohong Zhao,[a,*] Yu Hu,[a,*] and Yiwang Chen.[a]

[a] College of Chemistry and Chemical Engineering/Institute of Polymers and Energy Chemistry, Nanchang University, 999 Xuefu Avenue, Nanchang 330031, China.

E-mail: yuan@ncu.edu.cn (Z. Yuan), zhaoxh@ncu.edu.cn (X. Zhao).

Fax: +86 791 83969561; Tel: +86 791 83968703.

* Corresponding author.

Contents

1. Experimental Section

Materials and instruments. All the chemicals and materials were purchased from commercial suppliers. The UV-vis absorption was measured by a Perkin Elmer Lambda 750 spectrophotometer. The current density-voltage (*J*–*V*) characteristics of organic solar cells were measured using a Keithley 2400 Source Meter under simulated solar light (Abet Solar Simulator Sun 2000, 100 mW cm^2, AM 1.5 G).[1] The incident photon-to-electron conversion efficiency (IPCE) spectra were measured in an IPCE measuring system with an Oriel 70613NS QTH lamp. Atomic force microscopy (AFM) images were measured in the tapping mode with a NanoMan VS microscope.[2]

Device Fabrication. For the OSCs device, the conductive ITO substrates were sequentially cleaned with ultrasonication in detergent, water, acetone, and isopropanol. After drying the ITO substrates and treating the surface with UV ozone for 20 min, the poly(3,4-ethylenedioxythiophene):poly(styrenesulfonate) (PEDOT:PSS) was spin-coated at 4000 rpm for 40 s onto the ITO surface. After being baked at 150 ^oC for 20 min in air, the substrates were transferred into a nitrogen-filled glove box. Then the active layers were spun-coated from solutions of donor:acceptor (1:1 w/w) in $CHCl_3$ with a total concentration of 20 mg mL^{-1} (5% v/v chloronaphthalene). Anneal at 100 ^oC for 10 min. Afterward, 1 mg mL^{-1} of PDINO was spin-coated at 3000 rpm on the top side of the active layer. Ag (80 nm) were deposited by thermal evaporation under a vacuum chamber to complete the device fabrication. The effective area of one cell was 0.04 cm^2. The current-voltage (*J*–*V*) characteristics were measured by a Keithley 2400 Source Meter under simulated solar light (100 mW cm^{-2}, AM 1.5 G, Abet Solar Simulator Sun 2000). The incident photon-to-electron conversion efficiency (IPCE) spectra were detected on an IPCE measuring system (Oriel Cornerstone monochromator equipped with Oriel 70613NS QTH lamp). All the measurement was performed at room temperature under nitrogen atmosphere.[1]

SCLC device. The fabricated device procedure was the same as our previous reported references.[1] Hole and electron mobilities were measured using the space charge limited current (SCLC) method, with the hole-only device of ITO/poly(3,4-ethylenedioxythiophene): polystyrene sulfonate (PEDOT:PSS)/active layer/MoO_3/Ag and electron-only device

ITO/ZnO/active layer/PDINO/Al by taking a current-voltage curve in the range of -5.0 V~5.0 V. The SCLC mobilities were calculated by MOTT-Gurney equation, which is described by:

$$J = 9\varepsilon_0\varepsilon_r\mu V^2/8L^3$$

Where J is the current density, L is the film thickness of the active layer, ε_0 is the permittivity of free space (8.85×10^{-12} F m^{-1}), ε_r is the relative dielectric constant of transport medium, μ is the internal voltage in the device. $V = V_{appl} - V_r - V_{br}$, where V_{appl} is the applied voltage to the device, V_r is the voltage drop due to contact resistance and series resistance across the electrodes, and V_{br} is the built-in voltage due to the relative work function difference of the two electrodes.[3, 4]

2. Chemical structure of TBDPDI.

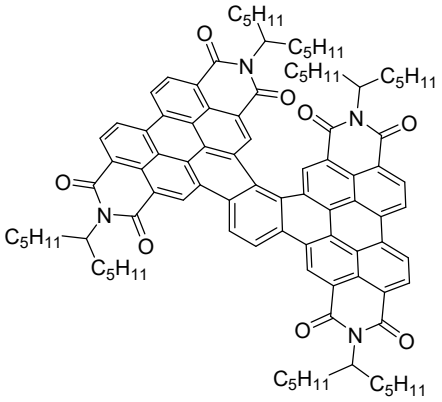

Fig. S1. Chemical structure of TBDPDI.

3. TGA curves of P(TBDPDI-TT) and P(TBDPDI-FTT).

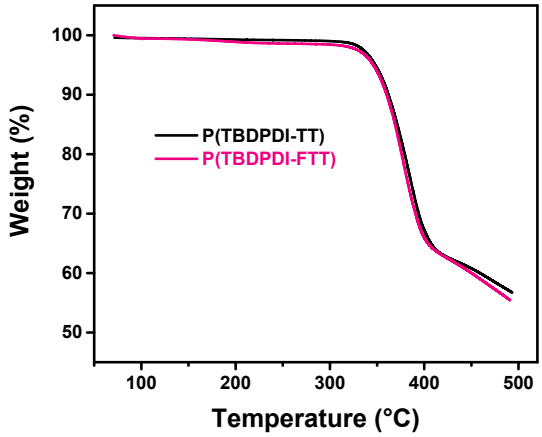

Fig. S2. TGA curves of P(TBDPDI-TT) and P(TBDPDI-FTT).

4. Cyclic voltammograms of P(TBDPDI-TT) and P(TBDPDI-FTT).

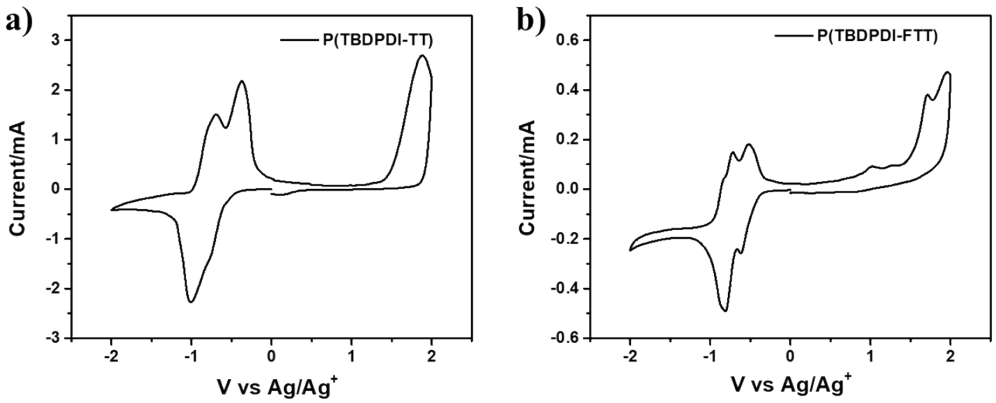

Fig. S3. Cyclic voltammograms of (a) P(TBDPDI-TT) and (b) P(TBDPDI-FTT).

As shown in Fig. S3, both of them exhibited multiple semi-reversible reduction peaks, indicating that they are capable of accepting multiple electrons. The highest occupied molecular orbital (HOMO) energy levels and LUMO energy levels are calculated by using the empirical equation of E_{HOMO} = -e(φ_{ox} + 4.80) (eV), E_{LUMO} = -e(φ_{red} + 4.80) (eV), the calculated HOMO/LUMO energy levels were -5.85/-3.81 and -5.90/-3.93 eV, for P(TBDPDI-TT) and P(TBDPDI-FTT), respectively. Compared to P(TBDPDI-FTT), P(TBDPDI-TT) has a higher LUMO and HOMO energy levels because the D block of P(TBDPDI-TT) is not fluorinated. The high LUMO energy level of the acceptor polymer facilitates the achievement of high V_{OC} in its photovoltaic devices.

5. Chemical structure, absorption spectra, and diagram of the device structure.

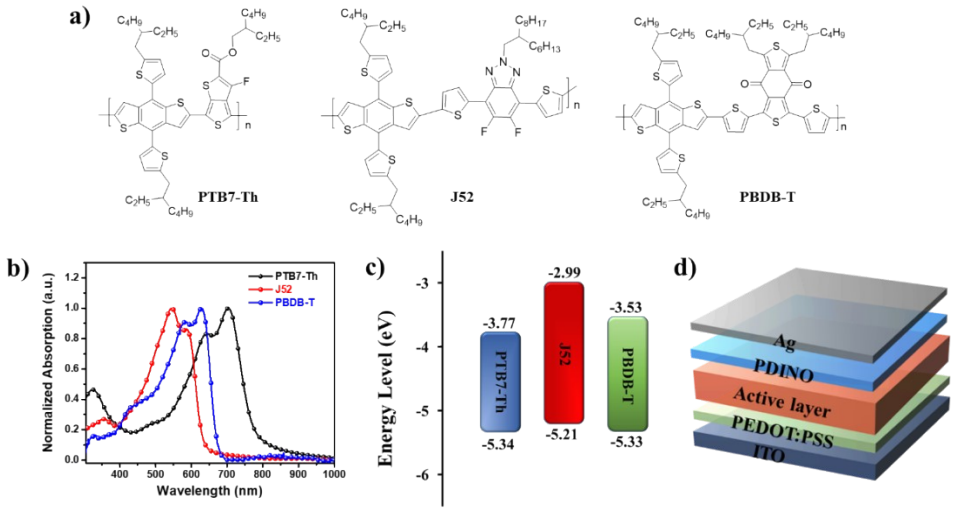

Fig. S4. (a) Chemical structures, (b) UV-vis absorption, and (c) energy level diagram of PTB7-Th, J52 and PBDB-T. (d) Diagram of the device structure.

6. The gel permeation chromatography (GPC) measurement of the polymers.

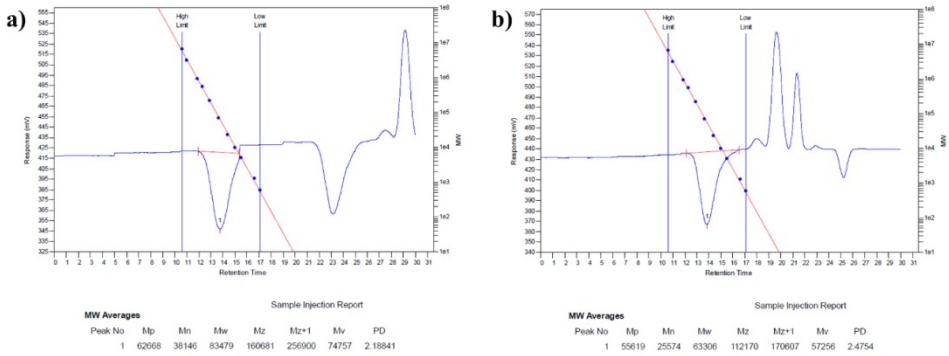

Fig. S5. The GPC measurement of the (a) P(TBDPDI-TT) and (b) P(TBDPDI-FTT).

7. Photovoltaic Device Performance Optimization.

Table S1. Photovoltaic properties of OSCs based on P(TBDPDI-TT) with different donor materials (D/A = 1:1, C = 20 mg mL^{-1}, thermal annealing at 100 °C for 10 min).

Blend films	V_{OC} (V)	J_{SC} (mA cm^{-2})	FF (%)	PCE[a] (%)
PTB7-Th:P(TBDPDI-TT)	0.979	11.15	38.93	4.25
J52:P(TBDPDI-TT)	0.969	8.07	46.65	3.65
PBDB-T:P(TBDPDI-TT)	1.011	3.79	59.70	2.29

[a] Optimum device efficiency.

Table S2. Photovoltaic properties of OSC based on conventional and inverted devices.

Devices	V_{OC} (V)	J_{SC} (mA cm^{-2})	FF (%)	PCE[a] (%)
Conventional	0.975	11.17	38.39	4.18
Inverted	0.953	9.35	35.70	3.18

[a] Optimum device efficiency.

Table S3. Photovoltaic properties of OSCs based on PTB7-Th:P(TBDPDI-TT) ($C_{PTB7\text{-}Th:P(TBDPDI\text{-}TT)}$ = 20 mg mL^{-1}) with different D/A ratios.

PTB7-Th:P(TBDPDI-TT)	V_{OC} (V)	J_{SC} (mA cm^{-2})	FF (%)	PCE[a] (%)
1.2:1	0.965	10.34	25.86	3.58
1:1	0.984	10.86	38.31	4.09
1:1.2	0.995	10.85	37.71	4.07
1:2	1.002	10.14	35.83	3.64

[a] Optimum device efficiency.

Table S4. Photovoltaic properties of OSCs based on PTB7-Th:P(TBDPDI-TT) (D/A = 1:1, $C_{PTB7\text{-}Th:P(TBDPDI\text{-}TT)}$ = 20 mg mL^{-1}) at different thermal annealing temperatures.

PTB7-Th:P(TBDPDI-TT)	V_{OC} (V)	J_{SC} (mA cm^{-2})	FF (%)	PCE[a] (%)
w/o	0.957	11.83	33.41	3.78
100 °C	0.978	10.75	35.27	3.71
120 °C	0.983	10.11	35.58	3.53
150 °C	0.977	10.06	35.33	3.47

[a] Optimum device efficiency.

Table S5. Photovoltaic properties of OSCs based on PTB7-Th:P(TBDPDI-TT) (D/A = 1:1, $C_{PTB7\text{-}Th:P(TBDPDI\text{-}TT)}$ = 20 mg mL^{-1}, thermal annealing at 100 °C for 10 min) by adding different solvent additives.

PTB7-Th:P(TBDPDI-TT)	V_{OC} (V)	J_{SC} (mA cm^{-2})	FF (%)	PCE[a] (%)
w/o	0.983	10.70	37.27	3.92
1% DIO	0.976	10.97	37.11	3.97
1% CN	0.970	11.21	38.03	4.13
1% DPE	0.982	10.59	35.57	3.70
1% NMP	0.989	10.09	36.19	3.61

[a] Optimum device efficiency.

Table S6. Photovoltaic properties of OSCs based on PTB7-Th:P(TBDPDI-TT) (D/A = 1:1, $C_{PTB7\text{-}Th:P(TBDPDI\text{-}TT)}$ = 20 mg mL^{-1}, thermal annealing at 100 °C for 10 min) by adding different contents of chloronaphthalene (CN).

PTB7-Th:P(TBDPDI-TT)	V_{OC} (V)	J_{SC} (mA cm^{-2})	FF (%)	PCE[a] (%)
w/o	0.978	11.63	35.72	4.05
0.5% CN	0.970	11.73	36.55	4.15
1% CN	0.964	12.00	37.56	4.33
3% CN	0.941	12.93	42.55	5.16
5% CN	0.936	13.75	44.19	5.69
10% CN	0.932	10.94	41.77	4.26

[a] Optimum device efficiency.

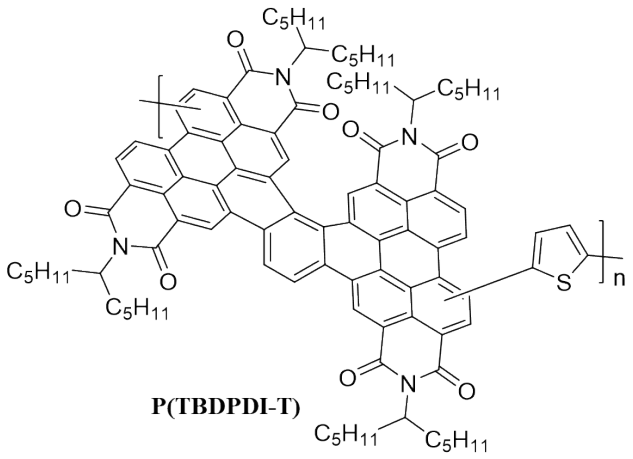

P(TBDPDI-T)

Table S7. Photovoltaic properties of OSC based on PTB7-Th:P(TBDPDI-T) (D/A = 1:1, $C_{PTB7\text{-}Th:P(TBDPDI\text{-}T)}$ = 20 mg mL^{-1}, 5% v/v CN, thermal annealing at 100 °C for 10 min)

Blend film	V_{OC} (V)	J_{SC} (mA cm^{-2})	FF (%)	PCE[a] (%)
PTB7-Th:P(TBDPDI-T)	0.945	8.27	36.12	2.82

[a] Optimum device efficiency.

Table S8. Photovoltaic properties of OSCs based on P(TBDPDI-FTT) with different donor materials (D/A = 1:1, C = 20 mg mL^{-1}, thermal annealing at 100 °C for 10 min).

Blend films	V_{OC} (V)	J_{SC} (mA cm^{-2})	FF (%)	PCE[a] (%)
PTB7-Th:P(TBDPDI-FTT)	0.893	11.89	31.35	3.33
J52:P(TBDPDI-FTT)	0.880	9.20	44.08	3.57
PBDB-T:P(TBDPDI-FTT)	0.921	6.51	47.97	2.87

[a] Optimum device efficiency.

8. NMR spectra of polymers.

8.1 ^{1}H NMR of P(TBDPDI-TT) in $CDCl_3$ (400 MHz).

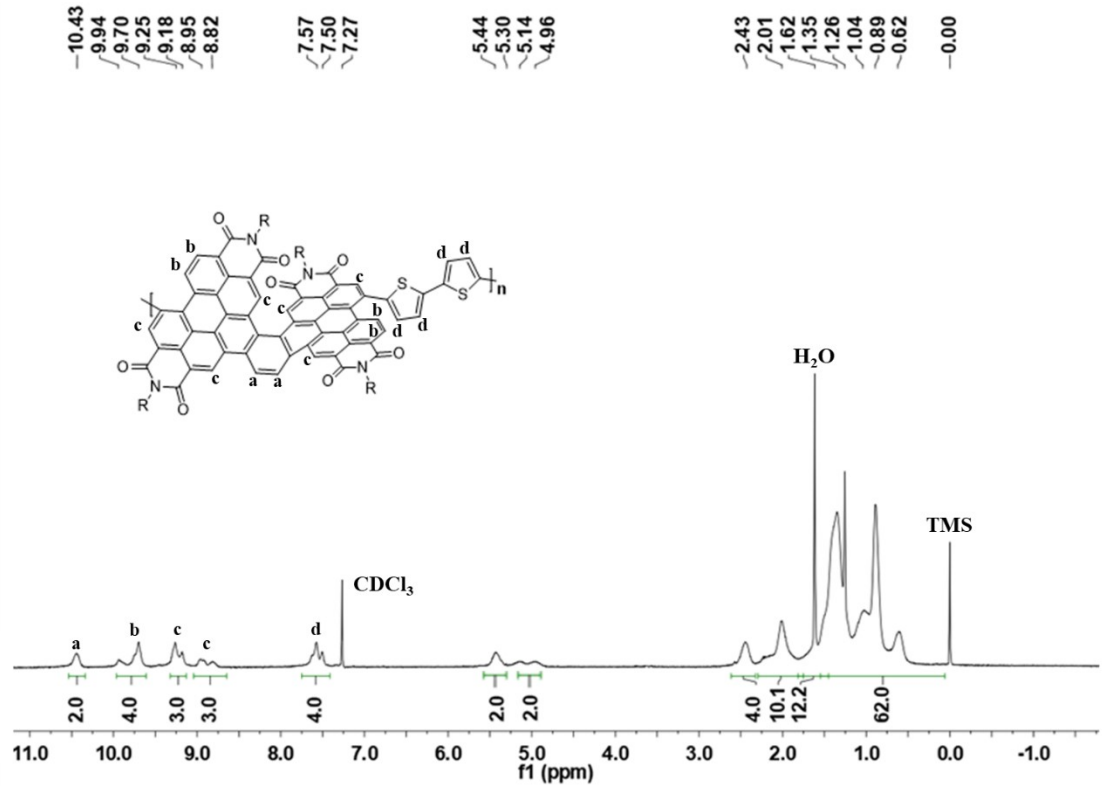

8.2 ^{1}H NMR of P(PTBDPDI-FTT) in $CDCl_3$ (400 MHz).

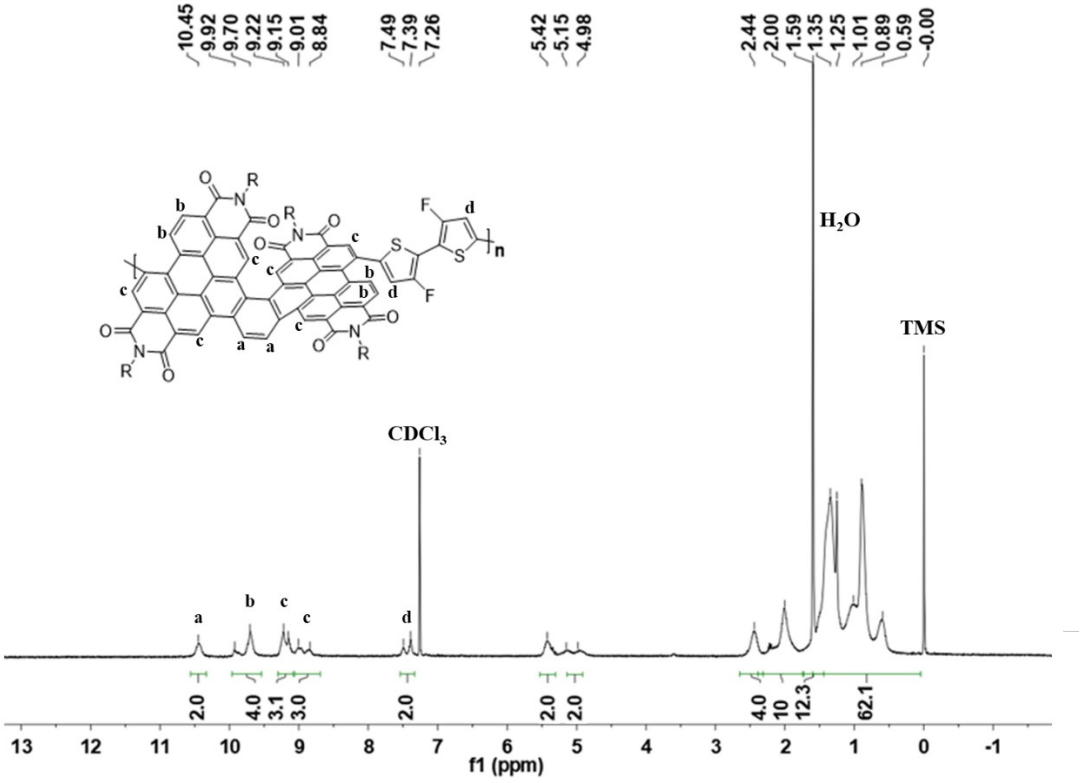

9. References

1 M. Hu, X. Zhao, G. Zhu, Y. Zhang, Z. Yuan, L. Wang, X. Huang, Y. Hu and Y. Chen, *Chem. Commun*., 2019, **55**, 703-706.

2 Y. Cho, T. L. Nguyen, H. Oh, K. Y. Ryu, H. Y. Woo, K. Kim, *ACS Appl. Mater. Interfaces*, 2018, **10**, 27757-27763.

3 A. Babel and S. A. Jenekhe, *J. Am. Chem. Soc*., 2003, **125**, 13656-13657.

4 M. M. Alam and S. A. Jenekhe, *Chem. Mater*., 2004, **16**, 4647-4656.